Analytic solutions throughout a period doubling route to chaos

Marko S. Milosavljevic, Jonathan N. Blakely, Aubrey N. Beal, and Ned J. Corron
Charles M. Bowden Laboratory, US Army Aviation and Missile Research, Development, and Engineering Center, Redstone Arsenal, Alabama 35898, USA
(Received 6 April 2017; published 29 June 2017)

We show examples of dynamical systems that can be solved analytically at any point along a period doubling route to chaos. Each system consists of a linear part oscillating about a set point and a nonlinear rule for regularly updating that set point. Previously it has been shown that such systems can be solved analytically even when the oscillations are chaotic. However, these solvable systems show few bifurcations, transitioning directly from a steady state to chaos. Here we show that a simple change to the rule for updating the set point allows for a greater variety of nonlinear dynamical phenomena, such as period doubling, while maintaining solvability. Two specific examples are given. The first is an oscillator whose set points are determined by a logistic map. We present analytic solutions describing an entire period doubling route to chaos. The second example is an electronic circuit. We show experimental data confirming both solvability and a period doubling route to chaos. These results suggest that analytic solutions may be a more useful tool in studying nonlinear dynamics than was previously recognized.

DOI: 10.1103/PhysRevE.95.062223

I. INTRODUCTION

Nonlinear dynamical systems can rarely be solved analytically. Historically, rapid progress in the study of nonlinear dynamics followed the widespread availability of digital computers. Numerical approximations to solutions of nonlinear systems were essential to the work of pioneers such as Lorenz, Feigenbaum, and Rössler [1–3]. So recent reports of chaotic dynamical systems with analytic solutions are quite unusual [4–7]. These analytic solutions have enabled an unprecedented degree of rigor in the characterization of chaotic dynamics. For example, exact conjugacies to known chaotic systems have been found, rigorously proving the chaotic nature of these solutions. Also, quantities used to describe chaotic dynamics that are usually estimated numerically, like the Lyapunov exponent, have been determined exactly. These successes raise the hope that greater analytic progress might be possible with familiar chaotic paradigms such as the Lorenz and Rössler systems. In this paper, we show how a simple modification of known solvable systems produces a classic nonlinear phenomenon hitherto unseen in any solvable system. Specifically, we derive analytic solutions describing the entire period doubling route to chaos shown in Fig. 1. This classic bifurcation sequence has been observed in countless chaotic systems in physics [8,9], chemistry [10,11], biology [12,13], engineering [14,15], and economics [16,17], but never before in a solvable system of the type we consider here.

The systems of interest here are described in terms of hybrid equations containing both a continuous-time linear system that oscillates about a set point and a rule for updating the value of the set point at discrete times [4–7,18]. Between instantaneous transitions of the set point, the evolution is purely linear and therefore directly solved. Updates to the set point occur such that the values of the system state at subsequent update times are related by a one-dimensional map. In previous studies, these maps were piecewise linear, e.g., the Bernoulli map or the tent map. Here we modify this scheme to obtain a smoothly nonlinear map. This change opens the door to a much greater variety of dynamical phenomena such as the period doubling route to chaos we focus on in this paper. We provide two illustrative examples of solvable systems that display period doubling bifurcations. The first is based directly on the logistic map and recapitulates its famous route to chaos. The second is a simple electronic circuit that provides a physical embodiment of the period doubling route to solvable chaos. Finally, we discuss period doubling in a larger class of possible solvable chaotic dynamical systems.

II. ANALYTIC SOLUTIONS FOR PERIOD DOUBLING

Consider the ordinary linear differential equation

$$\ddot{u} - 2\beta\dot{u} + (\omega^2 + \beta^2)(u - s) = 0, \tag{1}$$

where β and ω are constants. Let $\omega = \pi$ so that the natural period of Eq. (1) is 2. Let $\beta > 0$ so that the system is negatively damped (in contrast to dissipative kicked rotor models [19]). The variable $u(t) \in \mathscr{R}$ oscillates harmonically about a set point $s(t)$ that changes value only at discrete times in which $\dot{u} = 0$. At the ith such instant t_i let the value of s be updated according to the rule

$$s(t_i) = \frac{e^{\beta\pi/\omega}u(t_i) + f(u(t_i))}{1 + e^{\beta\pi/\omega}}, \tag{2}$$

where $f(u)$ is a function to be specified below. This value of s is retained until t_{i+1}, i.e., the next time when $\dot{u} = 0$. An analytic solution to Eq. (1) is an expression for $u(t)$ in terms of known functions that is consistent with some specified initial data for $u(0)$ and $\dot{u}(0)$. We now proceed to find such an analytic solution.

We first note that the harmonic oscillation of Eq. (1) ensures that $s(t)$ can only change values at instants regularly spaced by intervals of width equal to 1, i.e., half the natural period [20]. Without loss of generality, let $t = 0$ be such an instant. Then $s(t)$ must take the form

$$s(t) = \sum_{n=-\infty}^{\infty} s(n)\phi(t - n), \tag{3}$$

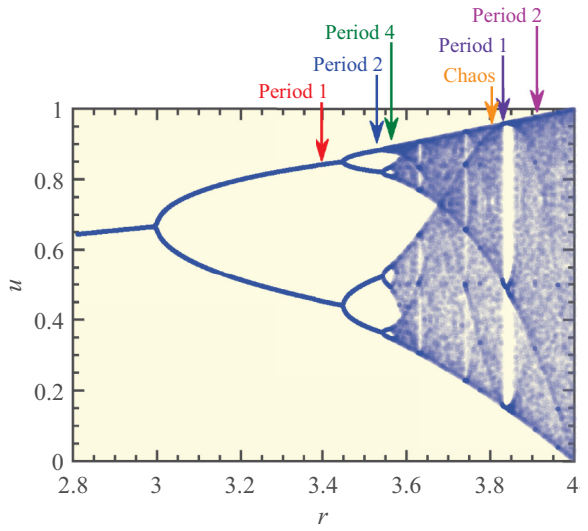

FIG. 1. Bifurcation diagram for the logistic map showing a period doubling route to chaos. This plot equally represents the bifurcations of the continuous-time dynamical system of Eqs. (1) and (2) where the values of u at set point update times are plotted. The periodicities of the continuous-time orbits shown in Fig. 2 differ from those of the logistic map and so are indicated above the plot.

where $\phi(t)$ is a square pulse of unit height and width 1 beginning at $t = 0$. Without yet knowing the values of $s(n)$ for any n except $n = 0$, we can formally view Eq. (1) as a linear system driven by this train of square waves. By the superposition principle, the response of the system to the train of pulses is equivalent to a sum of responses to each pulse in isolation. Therefore, the form of the solution must be

$$u(t) = \sum_{n=-\infty}^{\infty} s(n)Q(t-n), \tag{4}$$

where $Q(t)$ is the response to a single square pulse $\phi(t)$ [6]. This expression is analogous to the general solution of a linear ordinary differential equation. What remains in constructing an analytic solution is to determine the values of $s(n)$ such that Eq. (4) is consistent with the initial conditions.

In general, the values of $s(n)$ for all n can be determined as follows. It can be shown that the value $u(n+1)$ is related to $u(n)$ by the equation [5]

$$u(n+1) = -e^{\beta\pi/\omega}u(n) + (1 + e^{\beta\pi/\omega})s(n). \tag{5}$$

Setting $s(t)$ according to Eq. (2) we have

$$u(n+1) = f(u(n)). \tag{6}$$

For the initial condition $u(0)$, this map is iterated to produce a sequence of values $u(n)$ that can be substituted into Eq. (2) to obtain the values of $s(n)$ needed to make Eq. (4) a valid solution. Importantly, by choosing $f(u)$ to be a chaotic map we rigorously ensure that Eq. (1) has chaotic solutions. For example, with $f(u(n)) = ru(n)[1-u(n)]$ with r a fixed parameter, Eqs. (1) and (2) produce a continuous oscillation $u(t)$ whose samples at integer values of t are governed by the well known logistic map. A map can similarly be suspended in a continuous-time kicked rotor system [19]. We now explore

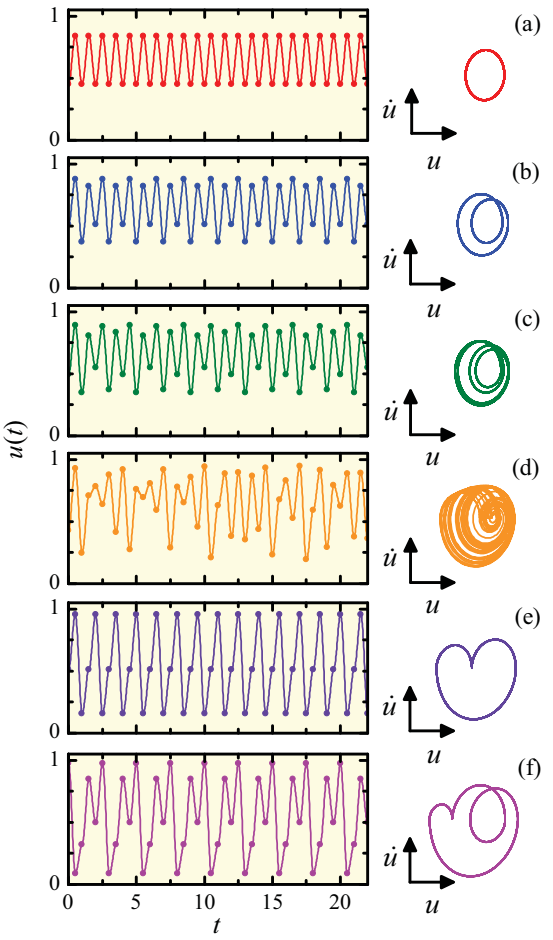

FIG. 2. Typical analytic solutions where the oscillation is (a) period 1 ($r = 3.4$), (b) period 2 ($r = 3.52$), (c) period 4 ($r = 3.562$), (d) chaotic ($r = 3.795$), (e) period 1 ($r = 3.82843$), and (f) period 2 ($r = 3.90558$). Points at which $\dot{u} = 0$ are marked by dots. To the right of each solution is the corresponding phase portrait.

the example of Eq. (1) with $f(u(n)) = ru(n)[1-u(n)]$ in detail.

The logistic map displays a sequence of period doubling bifurcations leading from stable oscillation to chaos that is treated in virtually every book on the subject of chaos. We can now observe this same phenomenon through the analytic solutions of Eqs. (1) and (2). From typical initial conditions, we have constructed solutions of Eqs. (1) and (2) displaying period-1, period-2, and period-4 oscillations as well as chaos, as shown in Fig. 2. Points where the slope of $u(t)$ is zero are indicated by dots. By design, these are also iterates of the logistic map. Along with each solution for $u(t)$, a phase portrait is presented that makes plain the periodicity.

Some features of these solutions are worth noting. The period doubling bifurcations of Eq. (1) occur at the same values of r at which bifurcations occur in the logistic map. Nevertheless, for a given value of r the periodicity of $u(t)$ (defined as the number of piercings of a Poincaré surface of section) is not the same as the periodicity of the corresponding logistic map iterates. At $r = 3.4$ the map is period 2, while $u(t)$ is period 1. At $r = 3.52$ the map is period 4, while $u(t)$ is period 2. In fact, because each extremum of $u(t)$ is an iterate of the

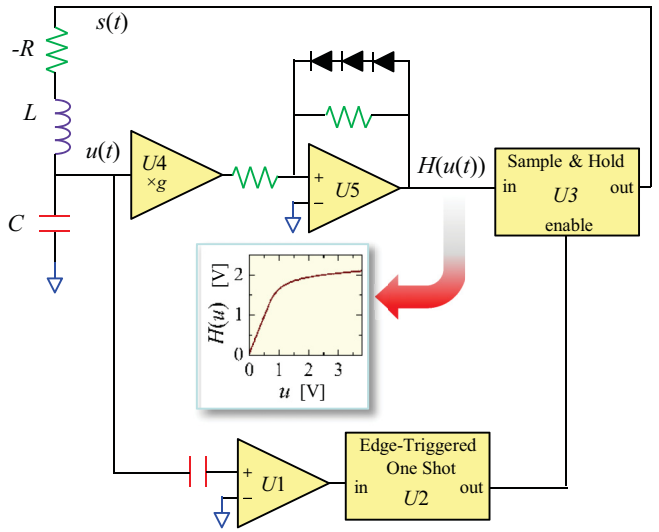

FIG. 3. Schematic diagram of an electronic circuit modeled by a solvable chaotic system with a period doubling route to chaos. The inset shows the measured nonlinear transfer function $H(u)$.

map, the period of the map throughout the sequence is twice the period of the continuous solution $u(t)$. Nonetheless, we observe the same accumulation point near $r = 3.57$ marking the onset of chaos in both bifurcation sequences. Beyond the accumulation point, the relation between the periods is even more surprising. For example, the period-3 orbit in the map coincides with a continuous orbit that is period 1. The period-5 orbit in the map corresponds to a period-2 orbit in Eq. (1). Thus, the dynamics of the hybrid system are not entirely dictated by the underlying map.

Interestingly, the analytic solution of Eq. (4) takes an especially concise form for two specific values of the parameter r. For both $r = 2$ and $r = 4$, exact solutions are known for the logistic map [21]. In these atypical cases, the values of $s(n)$ need not be determined by iteration of the logistic map, but can be calculated directly. For example, if $r = 4$ the values of $u(n)$ are given exactly by

$$u(n) = \sin^2(2^n \theta \pi), \tag{7}$$

where $\theta = \pi^{-1} \sin^{-1}[u(0)^{1/2}]$. These values can be substituted directly into Eq. (2) to obtain the $s(n)$ coefficients in Eq. (4). Any initial condition $u(0)$ yielding an irrational value of θ produces a chaotic orbit of the logistic map as well as a chaotic analytic solution to the hybrid system.

III. PERIOD DOUBLING IN A SOLVABLE CHAOTIC CIRCUIT

Besides the logistic map, many other choices of the function $f(u)$ are imaginable. We next consider a physically motivated choice of $f(u)$ arising from a simple electronic circuit implementation of Eqs. (1) and (2). Figure 3 shows a schematic diagram of the circuit. Specific implementation details are given in the Supplemental Material [22]. Here we provide a functional description of how the circuit works.

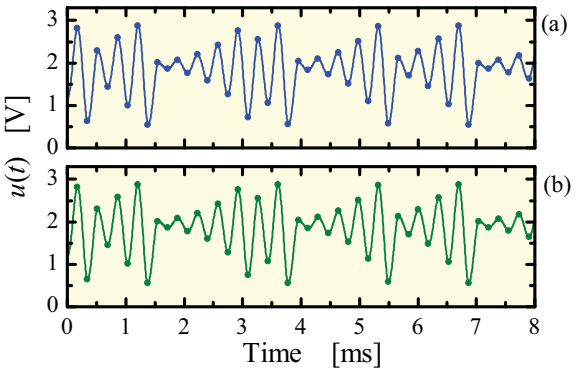

FIG. 4. (a) Typical time series of a measured circuit waveform in a chaotic region. (b) Corresponding analytic solution of the measured waveform. In both plots, dots indicate points where $\dot{u} = 0$.

The linear dynamics of Eq. (1) are implemented by a series capacitor-inductor-negative resistance circuit (with components labeled C, L, and $-R$, respectively). The voltage across the capacitor is the analog of the continuous state $u(t)$. The rest of the circuit regulates the set point value. A comparator ($U1$) monitors $\dot{u}$ for zero crossings and triggers a one shot ($U2$) to emit a narrow pulse. This pulse briefly enables a sample-and-hold chip ($U3$) whose updated output voltage drives the linear part of the system and is analogous to $s(t)$. The value of the set point at each update is supplied to the sample-and-hold chip by a nonlinear circuit consisting of two stages. The first is a linear amplifier ($U4$) with a gain g. The second is an amplifier ($U5$) whose output is limited by diodes in the feedback loop. The measured voltage transfer function H for the complete nonlinear circuit is shown in the inset in Fig. 3 for $g = 1.89$. At time t_n, the nth instant when $\dot{u}$ crosses zero, the set point value becomes $s(t_n) = H(t_n)$ and remains so until the next update.

A typical chaotic time series of $u(t)$, i.e., the voltage above capacitor C, is shown in Fig. 4(a). The gain $g = 1.89$. Points on the waveform are marked by circles at times t_n. A stored record of the values of $s(t_n)$ provides the coefficients needed to construct the corresponding analytic solution of the form of Eq. (4). The resulting constructed solution, shown in Fig. 4(b), closely matches the experimental waveform.

The points on the waveform where $\dot{u} = 0$ are shown as circles on a return map in Fig. 5. The map is a one-dimensional unimodal curve similar to the logistic map. Since set points for this circuit are directly determined by the nonlinear transfer function H, Eq. (2) can be solved for $f(u)$ to obtain

$$f(u) = (1 + e^{\beta\pi/\omega})H(u) - e^{\beta\pi/\omega}u. \tag{8}$$

The function $f(u)$ based on the measured values of $H(u)$ is shown by the blue line in Fig. 5. As expected, the return map iterates fall on this curve.

Figures 4 and 5 confirm that the circuit is accurately modeled by Eqs. (1) and (2) with set points determined by a unimodal map. We should therefore expect the circuit to display a period doubling route to chaos. By varying the gain g, we observe this very result as shown by values of $u(t_n)$ plotted in Fig. 6. This bifurcation plot begins with two-valued solutions corresponding to a continuous period-1 solution as

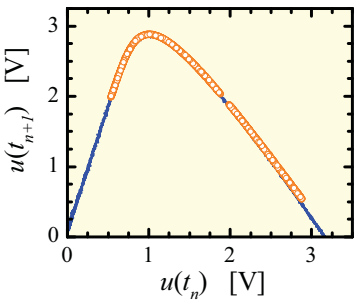

FIG. 5. Experimental return map for the chaotic electronic circuit of Fig. 3. The return values (indicated by circles) are drawn from the same data set as the time series in Fig. 4(a). The solid line is a curve derived from the measured transfer function shown in the inset in Fig. 3.

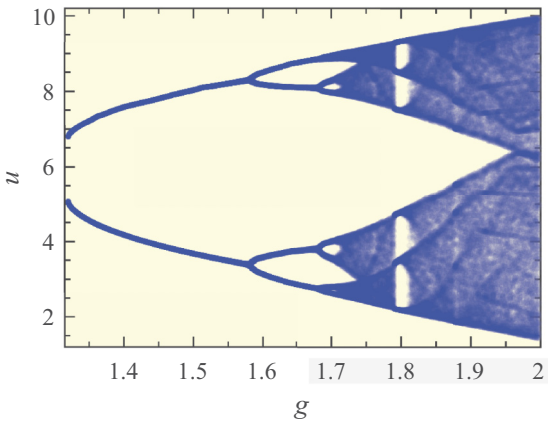

FIG. 6. Experimentally recorded bifurcation diagram for the circuit showing a period doubling route to chaos.

in Fig. 2(a). Two or three period doubling bifurcations are discernible before chaos set in as g is increased. This plot demonstrates an experimental observation of period doubling in a solvable chaotic oscillator.

The two examples of period doubling reported here do not exhaust the possible solvable system that may display this phenomenon. For example, an analytic solution for a hybrid system based on a first-order linear system was recently reported [7]. The role played by Eq. (1) in our examples is filled by the equation

$$\dot{u} = u - s. \tag{9}$$

The set point $s(t)$ changes only at discrete times as defined by an external clock. At the nth such instant t_n let the set point value be updated according to the rule

$$s(t_n) = \frac{e^T u_n - f(u_n)}{e^T - 1}, \tag{10}$$

where T is the clock period. Then, once again, the samples $u(t_n)$ satisfy the map of Eq. (6).

IV. CONCLUSION

In conclusion, we have shown how the update rule for the set points in solvable chaotic hybrid oscillators can be generalized to produce a classic phenomenon of nonlinear dynamics, the period doubling route to chaos. The scheme allows for any one-dimensional map to regulate the set point updates. Generation of an analytic solution to an initial-value problem requires only the iteration of the map, a process that is computationally more efficient than numerical integration of the differential equation. Generally, this approach may provide new insights into familiar nonlinear dynamical phenomena, such as intermittency, boundary crises, etc., where previously only numerical approximations were available. Additionally, these results may have technological relevance as chaotic analytic solutions have been put to practical use in designing optimal methods for communication and remote sensing in noisy environments [23–28].

[1] J. Gleick, *Chaos: Making a New Science* (Open Road Media, New York, 2011).
[2] E. N. Lorenz, *Essence of Chaos (Jessie and John Danz Lectures)* (CRC, Boca Raton, 1995).
[3] O. E. Rössler, Phys. Lett. A **57**, 397 (1976).
[4] N. J. Corron, Dyn. Contin. Discrete Impuls. Syst., Series A **16**, 777 (2009).
[5] N. J. Corron, J. N. Blakely, and M. T. Stahl, Chaos **20**, 023123 (2010).
[6] N. J. Corron and J. N. Blakely, Chaos **22**, 023113 (2012).
[7] N. J. Corron, R. M. Cooper, and J. N. Blakely, Chaos **26**, 023104 (2016).
[8] M. Giglio, S. Musazzi, and U. Perini, Phys. Rev. Lett. **47**, 243 (1981).
[9] G. Gibson and C. Jeffries, Phys. Rev. A **29**, 811 (1984).
[10] J.-C. Roux, Physica D **7**, 57 (1983).
[11] B. Peng, S. K. Scott, and K. Showalter, J. Phys. Chem. **94**, 5243 (1990).
[12] K. Aihara, G. Matsumoto, and Y. Ikegaya, J. Theor. Biol. **109**, 249 (1984).
[13] J. Halloy, Y.-X. Li, J. L. Martiel, B. Wurster, and A. Goldbeter, Phys. Lett. A **151**, 33 (1990).
[14] R. W. Rollins and E. R. Hunt, Phys. Rev. Lett. **49**, 1295 (1982).
[15] S. W. Teitsworth, R. M. Westervelt, and E. E. Haller, Phys. Rev. Lett. **51**, 825 (1983).
[16] W. A. Brock and C. H. Hommes, J. Econ. Dyn. Control **22**, 1235 (1998).
[17] H. Agiza and A. Elsadany, Physica A **320**, 512 (2003).
[18] T. Saito and H. Fujita, Electron. Commun. Jpn. 1 **64**, 9 (1981).
[19] R. Graham and T. Tél, Z. Phys. B **60**, 127 (1985).
[20] J. N. Blakely, R. M. Cooper, and N. J. Corron, Phys. Rev. E **92**, 052904 (2015).
[21] E. Schroder, Math. Ann. **3**, 296 (1870).
[22] See Supplemental Material at http://link.aps.org/supplemental/10.1103/PhysRevE.95.062223 for specific implementation details of the circuit.
[23] N. J. Corron, M. T. Stahl, and J. N. Blakely, Chaos **23**, 023119 (2013).

[24] H.-P. Ren, M. S. Baptista, and C. Grebogi, Phys. Rev. Lett. **110**, 184101 (2013).
[25] S. Zhang, J. Hu, and Z. He, Proceedings of the IET International Radar Conference 2013 (unpublished), pp. 1–5.
[26] L. Sun, J. Hu, C. Luo, and Z. He, in *Proceedings of the Second International Conference on Communications, Signal Processing, and Systems* (Springer, Berlin, 2014), pp. 541–548.
[27] N. J. Corron and J. N. Blakely, Proc. R. Soc. A **471**, 20150222 (2015).
[28] H.-P. Ren, C. Bai, J. Liu, M. S. Baptista, and C. Grebogi, Chaos **26**, 083117 (2016).